2010 NDIA GROUND VEHICLE SYSTEMS ENGINEERING AND TECHNOLOGY SYMPOSIUM
MODELING & SIMULATION, TESTING AND VALIDATION (MSTV) MINI-SYMPOSIUM
AUGUST 17-19 DEARBORN, MICHIGAN

NEW INTEGRATED TESTING SYSTEM FOR THE VALIDATION OF VEHICLE-SNOW INTERACTION MODELS

Jonah H. Lee
Thomas H. Johnson
Daisy Huang
University of Alaska Fairbanks
Fairbanks, AK

Stephen Meurer
US Army Cold Regions Test Center
Fort Greely, AK

Alexander A. Reid
Bill R. Meldrum
US Army Tank Automotive Research, Development and Engineering Center
Warren, MI

ABSTRACT

A new integrated testing system for the validation of stochastic vehicle-snow interaction models is presented in this paper. The testing system consists of an instrumented test vehicle, vehicle-mounted laser profilometer and a snow micropenetrometer. The test vehicle is equipped on each tire with a set of 6-axis wheel transducers, and a GPS-based data logger tracks vehicle motion. Data is also simultaneously acquired from the sensors from the test vehicle's Electronic Stability Program. The test vehicle provides measurements that include three forces and moments at each wheel center, vehicle body slip angle, speed, acceleration, yaw rate, roll, and pitch. The profilometer has a 3-D scanning laser and an Inertial Measurement Unit to compensate for vehicle motion. Depth of snow cover, profile of snow surface and wheel sinkage can be obtained from the profilometer. The snow micropenetrometer measures the strength of the snow cover before and after vehicle traversal. Preliminary results, including traction, drawbar pull, vehicle states, snow profiles and snow material properties from recent field tests on natural snow cover are presented, demonstrating the capability and potential of the testing system.

INTRODUCTION

The interaction of a vehicle with a soft terrain plays a significant role in the mobility, maneuverability, energy and power consumption as well as the safety of the vehicle. The material properties and the profile of naturally occurring terrains, such as snow and soils, are not deterministic but statistical in nature, necessitating the development and validation of stochastic vehicle-terrain interaction models that can be used to study the reliability of ground vehicles, among other applications.

Properties of natural snows vary depending on atmospheric conditions during formation, such as temperature and saturation, and localized ground conditions during metamorphosis, such as ground temperature, air temperature,

humidity, and sun and wind exposure. Different types of snow show different responses to loading and deformation, depending on the snow microstructure. Consequently, the mechanical properties of snow, important for vehicle-snow interaction, need to be studied in a statistical framework [1].

In recent years, extensive efforts in the modeling of tire-snow interaction have been carried out at the University of Alaska Fairbanks in conjunction with collaborators [2-6]. For deterministic modeling, the focus has been on a physics-based approach [2-3] rather than mostly empirical approach employed in the past; also both longitudinal slip and lateral slip (slip angle) have been studied, reflecting more realistic vehicle maneuvers. Based on the deterministic models, stochastic models have been developed [5-6] such that the influence of the uncertainties of parameters, such as material properties and snow depth, on vehicle performance can be quantified statistically. Due to a lack of comprehensive data on tire-snow interaction relevant to these models, only very limited validation of the models has been possible.

In this paper, we present a new integrated testing system for the validation of stochastic vehicle-snow interaction models such that terrain profile, terrain material properties, vehicle states as well as vehicle responses can be obtained and correlated.

The paper is organized as follows. Essential components of vehicle-snow interaction model are first discussed with key parameters defined. Each sub-system of the integrated testing system is then discussed in detail. Finally, test procedures and preliminary results are presented to demonstrate the capability and potential of the testing system.

VEHICLE-SNOW INTERACTION

Figure 1 shows important variables for vehicle-snow interaction in the longitudinal direction, i.e., when the vehicle maintains a straight heading with a velocity v. For a snow cover with initial depth (h_s), and a tire with deformed radius (*r*), when a torque (T_{app}) and vertical load (F_z) are applied to the tire, the deformation of snow (or the sinkage of tire) is z_0. For each point of the tire in contact with snow, there exists a normal stress (σ_n) and a shear stress (τ). The resultant force due to the stresses in the vertical direction is balanced by F_z. The traction force $F_{\tau x}$ is due to the applied torque and can be calculated as [7]

$$F_{\tau x}=\frac{T_{app}}{r} \tag{1}$$

The traction is also the horizontal component of the resultant force due to τ. The horizontal component of the resultant force due to σ_n, on the other hand, gives the motion resistance R_x that the vehicle needs to overcome. The vector sum of $F_{\tau x}$ and R_x is the drawbar pull F_x:

$$F_x=F_{\tau x}+R_x \tag{2}$$

When the traction force is larger than the motion resistance, the drawbar pull is positive; otherwise, it is negative.

The essential components of a tire-snow interaction model [2] are illustrated in Fig. 2. The inputs to the model are the vertical load (F_z), snow depth (h_s), longitudinal slip (i_x), as well as the cohesion (c) and friction angle (φ) of snow. Being a porous material, the mechanical properties of snow depend on the hydrostatic pressure such that the shear stress (τ) and normal stress (σ_n) are related via pressure-dependent yield criterion such as the Mohr-Coulomb or Drucker-Prager criterion where the cohesion and friction angle are typically used. The longitudinal slip (i_x) is defined as

$$i_x=1-\frac{v}{r\omega}$$

where ω is the angular velocity.

The outputs of the model are tire sinkage z_0, the drawbar pull F_{zx}, and traction $F_{\tau x}$. The motion resistance can then be calculated using equation (2). In the model [2], the pressure-sinkage relationship relates the normal stress (σ_n) to sinkage, which is a function of snow depth and material properties. Similarly, the longitudinal slip (i_x), induces a shear displacement (j_x), which is related to the shear stress (τ) via the shear stress-shear displacement relationship. The shear stress is also a function

of the normal stress (σ_n) due to the pressure-dependent nature of the material properties. The load-sinkage equation is essentially an equilibrium balance relating the applied load to interfacial stresses.

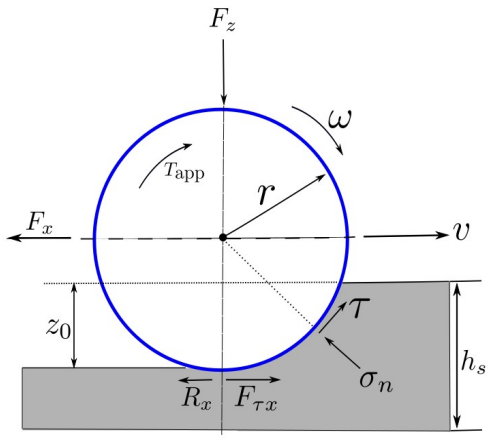

Figure 1: Definition of tire-snow interaction parameters.

INTEGRATED TESTING SYSTEM

The integrated testing system consists of an instrumented test vehicle, a high-resolution terrain profilometer and a high-resolution snow micropenetrometer. For the inputs and outputs shown in Figs. 1-2, the test vehicle measures the vertical load (F_z), the drawbar pull (F_x), the applied torque (T_{app}) which can be used to calculate the traction force ($F_{\tau x}$) via equation (1), the angular velocity of the wheel (ω), and the linear speed (v) of the vehicle. Snow depth (h_s) and tire sinkage (z_0) can be measured by the terrain profilometer. The mechanical properties (c , φ) can be derived from snow micropenetrometer measurements. The micropenetrometer can also be used to measure snow depth and tire sinkage but only manually, which is laborious. A description of each component of the testing system follows.

Instrumented Ground Vehicle

The test vehicle has an integrated antilock brake, traction control and stability control system (Electronic Stability Package, or, ESP) with 245/65 R17 tires. The ESP receives a multitude of inputs from sensors throughout the vehicle. Included are individual wheel speeds, accelerator pedal position, vehicle speed, yaw rate, lateral acceleration, steering wheel angle and brake input. The ESP can reduce engine power and apply braking independently to each wheel in an attempt to maintain the driver's intended path. The ESP communicates with other control units via the power train CANbus (Controller Area Networking bus). This bus is also referred to as the CanC bus and is the means by which the transmission, engine, and brake control units are networked. The CanC bus operates a baud rate of 500,000 bps, and the CAN messages follow the Standard CAN format. Update rate is determined by the vehicle and varies depending on the channel.

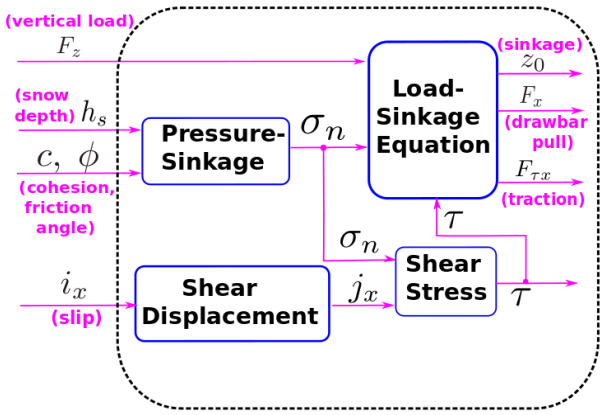

Figure 2: Essential components of tire-snow interaction model.

The vehicle is fitted with the Measuring Wheel system shown in Fig. 3. This system consists of four force and moment sensing wheels and the associated electronics. Each wheel has four load cells mounted between the hub and rim. These transducers measure forces in and moments about the *x*, *y*, and *z* directions. Additionally, the wheels' angular positions and angular velocities are measured. Data from these transducers are transmitted to the onboard electronics wirelessly through a ring antenna located at the hub of each

wheel. These electronics correct for the rotating reference frame and provide the forces and moments in near real time. Additionally, these electronics are configured as node on the vehicle CanC bus. All system channels are updated at 80 Hz.

A GPS-based system provides data on slip angle, pitch, and roll and uses three antennas mounted on the roof of the test vehicle. In addition, the system gathers traditional GPS information such as time and location. The system is also configured as a node on the CanC bus with channels updated at 20 Hz.

CAN signals from the vehicle, the measuring wheel system and GPS system are combined in CAN breakout box. CAN messages are monitored with a High Speed CAN Interface and the data acquired using a custom program running on a standard laptop. During a test, all decoded channels are monitored and displayed in real time. Furthermore, all CANbus data are recorded for post processing and analysis.

Terrain Profilometer

The U.S. Army Tank Automotive Research, Development and Engineering Center (TARDEC) possesses and uses a 3-D terrain laser scanning system (profilometer – see Fig. 4) to measure terrain surfaces with millimeter accuracy. The profilometer is based upon a HMMWV vehicle. It consists of a scanning laser mounted above and forward, accelerometers and inertial measurement units mounted behind the laser, a differential GPS system and two computers to collect the Inertial Measurement Unit (IMU), GPS and laser data.

Profiling a terrain consists of 3 steps:

1. Driving and scanning the terrain using the scanning laser, IMU, accelerometers and the differential GPS unit (both a base station and the remote unit on the profilometer).
2. Combining the GPS solution with the IMU and accelerometers to account for vehicle motions (roll, pitch, yaw) during the data collection phase.
3. Post-processing of the laser data with the vehicle history data using several software packages.

The laser is mounted 2 meters above the ground and performs a 4m wide scan consisting of 940 data points, equally angularly spaced (0.0957° apart during the scan). This provides smaller linear spacing towards the center of the scan (approximately 3.3 mm spacing) and larger spacing between points towards the edges (~6.6mm), as shown in Fig. 5. Once a scanning run is complete, we move onto step 2 in the process. As shown in Fig. 6, the GPS solutions from the base station and the profilometer are combined, removing GPS drift errors in the process. They are then combined with the IMU solution using a Kalman filter, providing the corrected vehicle position and orientation.

Figure 3: Instrumented ground vehicle.

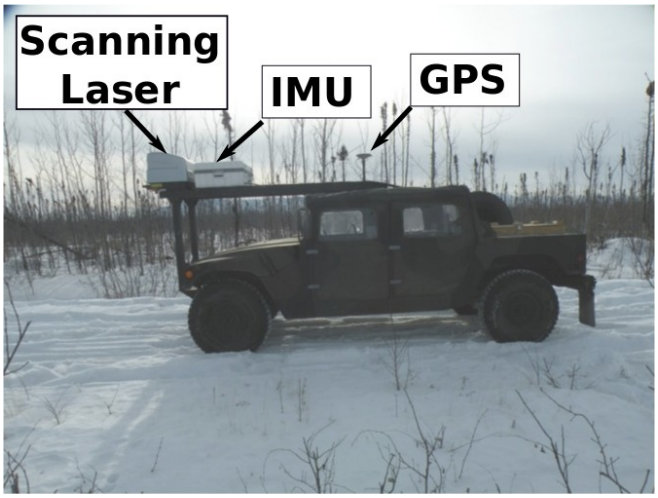

Figure 4: Profilometer in Alaska.

To determine the laser orientation and height, accelerometers are mounted on the same frame as the laser and IMU package, and their output is filtered and double integrated. The laser scan data is taken as is recorded.

Final post-processing of the data takes place off-line from the profilometer. Using software scripts, the Inertial Navigation System (INS) solution, laser orientation and height along with the scan data are filtered and mathematically combined into ground truth. Examples of the profiles obtained from the profilometer are shown in Fig. 7.

Snow Micropenetrometer

The cone penetrometer [8] is composed of an indentation cone mounted on a shaft, which serves as a lead screw to move the cone up and down. On the cone is a force transducer with a range of 0–500 N and a resolution of 0.01 N, and the entire assembly is mounted onto two support legs, as shown in Fig. 8.

The cone penetrometer records the force experienced by the cone tip during penetration into the snow. This output is utilized to calculate the strength of the snow. Because the diameter of the penetrometer tip is only 5 mm, and the force transducer takes readings at 20 mm/s at approximately 5000 Hz (resulting in about 250 samples per mm of snow depth), the snow properties can be measured and compared for highly localized areas, such as within a tire track versus adjacent to a tire track.

An algorithm developed in [9] takes the force data from the penetrometer and inverts the signal to determine properties such as average structural element length, deflection at rupture, and compressive strength, for a user-selected group of data points. Of these outputs, the compressive strength is of the highest interest.

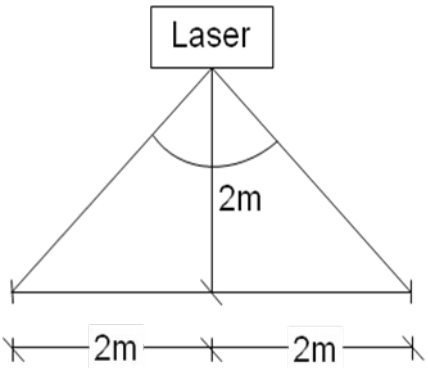

Figure 5: Laser scanner.

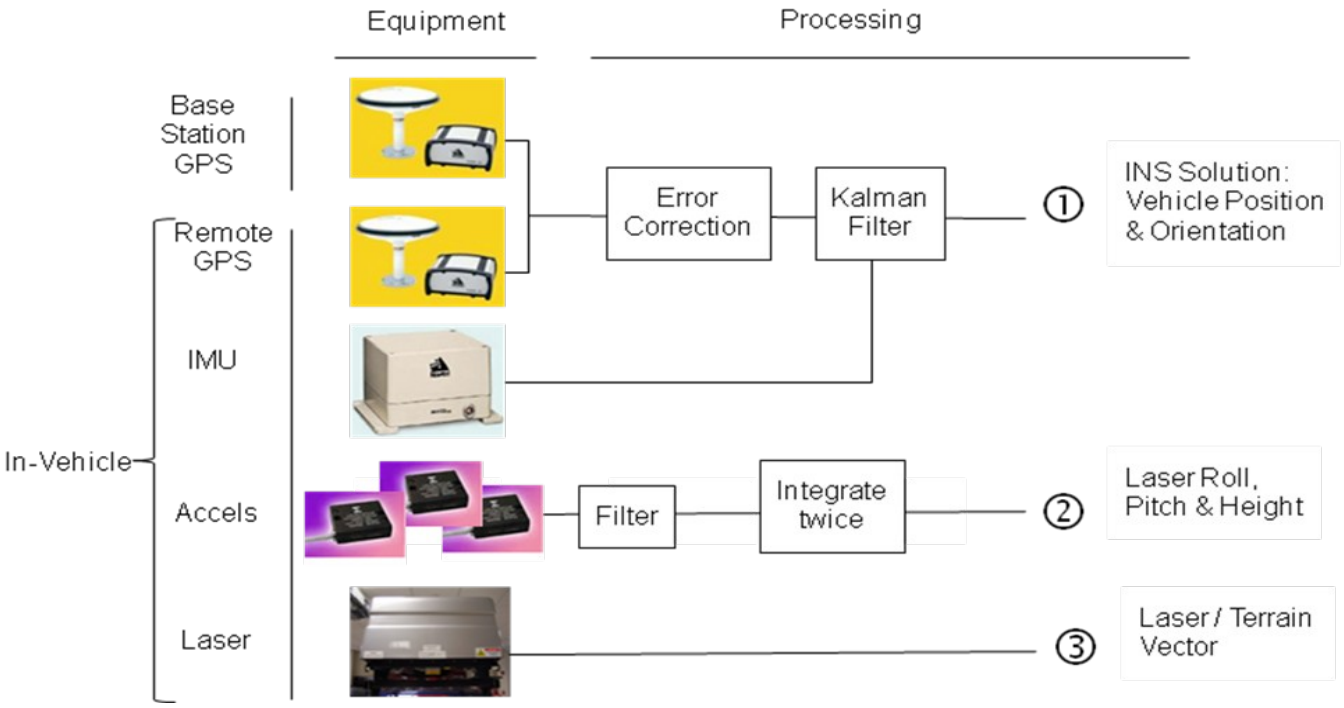

Figure 6: Signal processing flowchart.

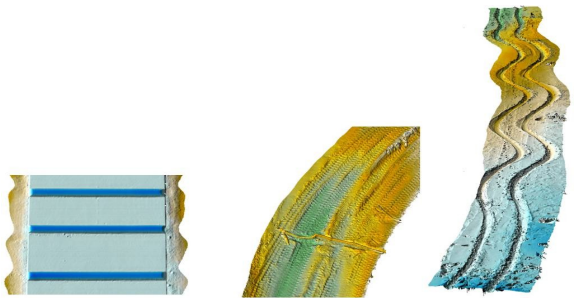

(a) (b) (c)

Figure 7: (a) 7.62 cm (3") half-Rounds, (b) segment of a trail, and (c) slalom pattern in snow.

The snow penetrometer also live-calculates and reports another parameter called the Texture Index (TI), which is average snow grain size in microns divided by the snow density in kg/m^3. Therefore, if the density can be obtained from an independent method, the TI gives the user average grain size at a locale. The TI sampling rate is approximately 10 Hz, so approximately 2 mm of snow depth are encompassed in each TI data point.

Before each set of tests, air temperature and ground temperature were recorded, and a sample of virgin snow was collected and brought to the laboratory in a cooler and scanned using 3D X-ray computed tomography (CT). The CT scan gave a 3D picture of the snow, from which parameters such as density and average grain size can be calculated.

TEST PROCEDURES

The integrated testing system was deployed in March, 2010 near Delta Junction, Alaska. Various tests of the

instrumented vehicle were conducted on an automotive test track to obtain baseline data of the vehicle [10]. For snow testing, the site was selected based on whether there is a sufficient amount of natural snow on the ground and whether the site is sufficiently long and wide to allow continuous testing to accommodate the instrumented vehicle as well as the profilometer. Various vehicle maneuvers were executed such as low-speed straight driving, accelerate-brake driving as well as slalom driving; the test vehicle's ESP was turned off during the tests. The general sequence of testing is as follows:

1. Snow micropenetrometer data is first collected on virgin snow before vehicle traversal.
2. The test vehicle then executes desired maneuvers followed by the terrain profilometer; care was taken so that the wheels of the profilometer do not overlap the tracks left by the instrumented vehicle.
3. Finally, snow micropenetrometer data is again collected on tire tracks after vehicle traversal.

RESULTS

In this section, we present preliminary results using the integrated system. Vehicle data is from the accelerate-brake test for the left-front wheel. Accompanying data from the profilometer and tire sinkage in the tire track are presented next. Finally, the characteristics of the snow layer including strengths before and after vehicle traversal are discussed.

Time history of vehicle response

This subsection presents results of the time history of vehicle response due to the accelerate-brake maneuver. The Savitzky-Golay method was used to smooth the raw data.

Figure 9 shows the comparison of wheel speed measured by the test vehicle's wheel speed sensor and the vehicle speed measured by the GPS sensor. The GPS sensor shows that the accelerate-brake maneuver was well executed by the driver. The wheel speed during the acceleration phase shows a higher value than that obtained from the GPS sensor indicating that the wheel is slipping and losing traction; i.e., the longitudinal slip is high. This can be seen from Fig. 10. The slip can be as high as 0.9, approaching the full slip value of 1.0. Fig. 10 also shows a large range of values of the longitudinal slip, desirable for future validation of models. Fig. 11 shows the vertical load (F_z) and the applied torque (M_y or T_{app}) as a function of time; F_z ranges between approximately 4 kN and 7 kN, indicating the dynamic nature of the vehicle response. M_y as a function of time changes sign from driving torque to braking torque, corresponding to the accelerate-brake driving maneuver. Fig. 12 shows the traction force ($\frac{M_y}{r}$) and the drawbar pull (F_x) as a function of time; the distance between the two curves indicates the motion resistance as a function of time. As expected, the traction force is always higher than the motion resistance which can be as high as 1.5 kN, indicating the importance of the mechanical properties of snow in vehicle performance.

Figure 8: Snow micropenetrometer.

Tire sinkage

Figure 13 shows the contour plot of the *z*-coordinate (elevation) of a stretch of snow cover (6.5m x 0.7 m) after vehicle traversal for the accelerate-brake maneuver; the red color indicates higher elevation, and the blue color indicates lower elevation. The difference between the elevation of the highest point and that of the lowest point for a given longitudinal distance is defined as tire sinkage; moving average of a window of three data points in the longitudinal direction was used to smooth the data. The sinkage ranges from 8.5-13 cm.

Mechanical properties of snow

Snow was sampled before and after the vehicle had traversed it. It was determined that the snow was a wind-sintered, fine-grained layer over an unsintered layer that could either be fine or coarse, depending on location. The mechanical properties obtained from the snow were tabulated for use in vehicle-snow interaction models.

For virgin snow, the density calculated from the CT scans varied from 293 kg/m^3 in the soft layer beneath the surface to 442 kg/m^3 in the windblown, sintered top crust.

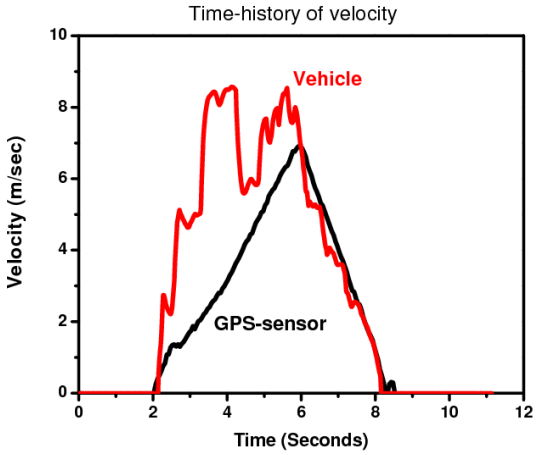

Figure 9: Comparison of wheel speed and vehicle speed from GPS sensor.

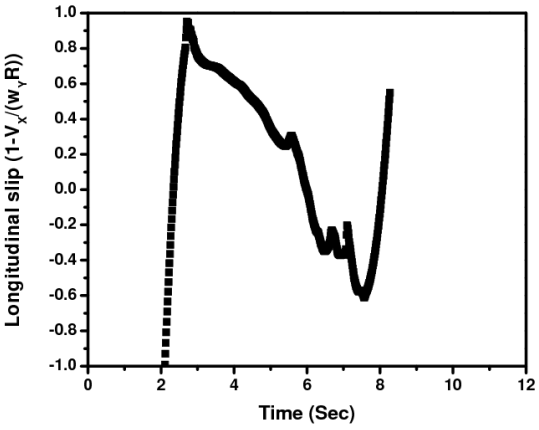

Figure 10: Longitudinal slip (i_x) versus time.

The snow penetrometer records the snow strength as the cone tip penetrates each snow layer. An example of one reading is shown in Fig. 15, which is a depiction of a penetrometer test into virgin snow. The origin of the penetration depth in Fig. 15 is the location where the penetrometer first makes contact with the snow. For the first 10 mm or so, the cone tip penetrates the top crust that has experienced some melting and refreezing. From 10 to about 95 mm depth, the snow is soft and offers little resistance to indentation. Then there is a much harder, denser layer beneath that. And so on.

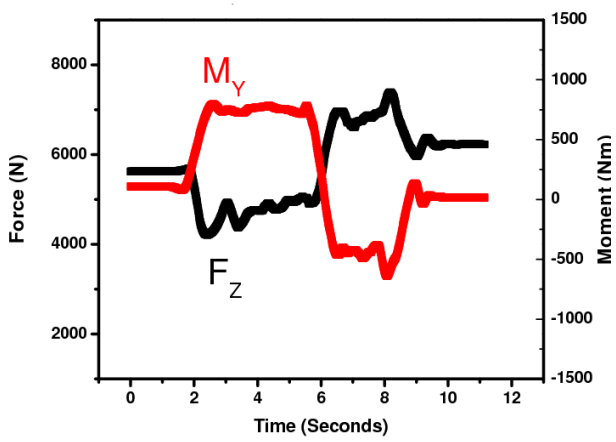

Figure 11: Applied torque (M_y) and vertical load (F_z) as a function of time.

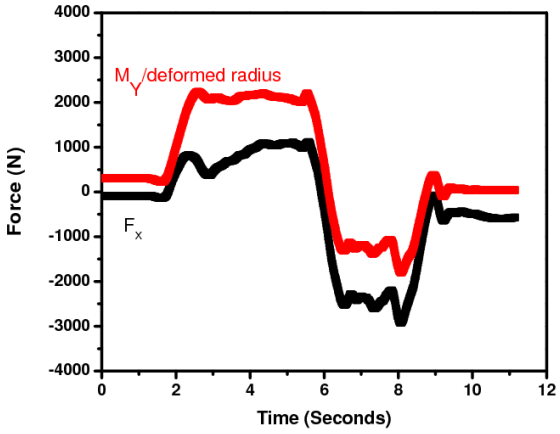

Figure 12: Traction force ($F_{tx}=M_y/r$) and drawbar pull (F_x) as a function of time.

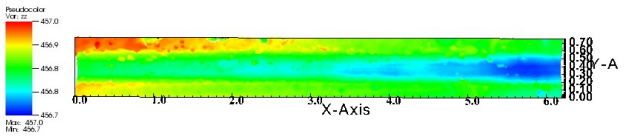

Figure 13: Contour plot of the elevation of snow cover (6.5 m x 0.7 m) after vehicle traversal. Red is higher elevation, blue is lower elevation. Vehicle motion is from left to right (*x*-direction).

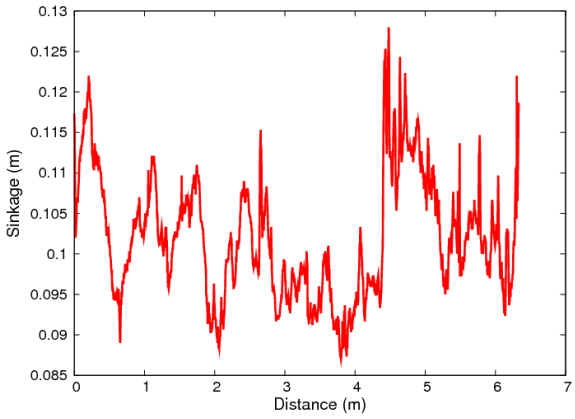

Figure 14: Tire sinkage versus distance of vehicle travel.

Figure 16 is a depiction of a penetrometer test into snow that has been traversed by the test vehicle's tire. In this example, the resistance force increases as the cone tip penetrates deeper into the compacted snow. In this manner, the depth of each layer of snow can be determined, and each layer can be analyzed separately.

For each layer, the compressive strength was calculated using the algorithm in [8]. This second data set is also plotted in Figs. 15-16, alongside the penetration force. This reflects that when the penetration force is higher, the snow has a correspondingly higher compressive strength.

The texture indices varied from 2.20 in a virgin (uncompressed) hard top crust to 3.66, in a tire track after vehicle traversal through deep, soft snow. Texture index is obtained as a function of depth for a localized area. For

example, the texture index from the same snow as in Fig. 15 is shown below in Fig. 17. As Fig. 15 showed, this snow has an abrupt change in properties at a depth of about 95 mm.

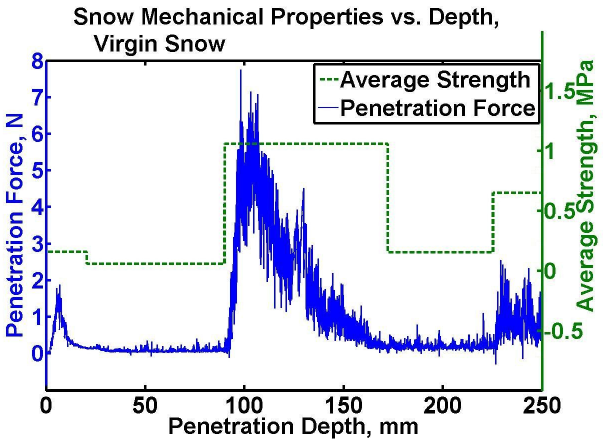

Figure 15: Penetration force from snow micropenetrometer and average compressive strength versus penetration depth for virgin snow; note that the snow is layered.

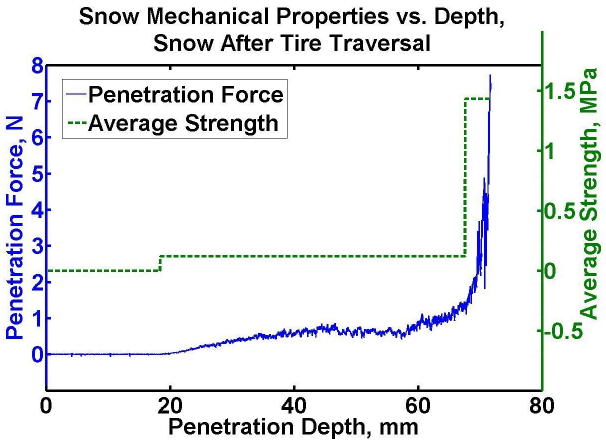

Figure 16: Penetration force from snow micropenetrometer and average compressive strength versus penetration depth for snow after tire traversal.

This is reflected in the texture index, with higher density resulting in both a higher penetration force and a lower texture index. Texture index was a less valuable parameter for characterizing snow after tire traversal.

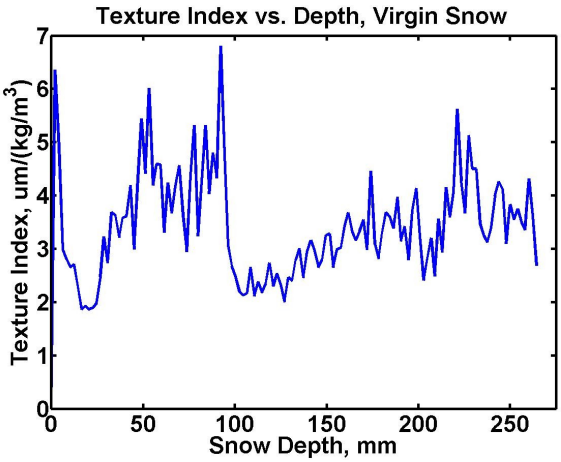

Figure 17: Texture index versus depth for virgin snow.

DISCUSSIONS AND CONCLUSIONS

It should be noted that the data obtained from the testing system represent the more realistic situation of varying vertical load, snow depth, longitudinal slip and mechanical properties of snow commonly encountered for vehicles over snowy terrain. The instrumented vehicle is able to obtain traction, drawbar pull and motion resistance at the same time, and *on the same snow,* providing more realistic data. In addition, the accelerate-brake maneuver is effective in that it is able to capture a wide of range of longitudinal slip values in a single run. The profilometer can obtain high-resolution terrain data over a large area in a short period of time. This enables tire sinkage to be calculated accurately and efficiently. The terrain profile of virgin snow can be used to validate stochastic terrain profile models in the future. Snow depth, another crucial parameter, can be obtained by profiling the terrain twice, once with snow and once without. Snow depth, which can also be used to validate stochastic snow depth models, will be obtained in the near future.

Snow samples were taken, and snow was characterized, at representative locations before and after traversal by the test vehicle. The mechanical properties measured and calculated from the snow penetrometer were recorded, compiled, and analyzed for input into the vehicle-snow interaction models.

In conclusion, the integrated testing system performs well to obtain all the important parameters needed for the validation of stochastic tire-snow interaction models. Although only preliminary data for the longitudinal motion of vehicle are presented, the testing system has a strong potential to obtain data for combined (longitudinal and lateral) slip as well as for more sophisticated maneuvers.

ACKNOWLEDGEMENTS

The authors gratefully acknowledge the support of this work by the U.S. Army TACOM Life Cycle Command under Contract No. W56HZV-08-C-0236, through a subcontract with Mississippi State University. This work was performed in part for the Simulation Based Reliability and Safety (SimBRS) research program. Any opinions, findings and conclusions or recommendations expressed in this material are those of the authors and do not necessarily reflect the views of the U.S. Army TACOM Life Cycle Command.

REFERENCES

[1] Yuan, H., Lee, J.H., Guilkey, J.E., "Stochastic reconstruction of the microstructure of equilibrium form snow and computation of effective elastic properties", *J. Glaciology* (in press).

[2] Lee, J.H. , Liu, Q., "Upper bound indentation theory for Snow-Depth Dependent Sinkage Calculation", Proceedings of the 15th International Conference of the ISTVS, Hayama, Japan, 2005.

[3] Lee, J.H., "A new indentation model for snow", *J. Terramechanics*, 46 (2009), 1-13.

[4] Lee, J.H., "Longitudinal interfacial forces of the interaction of a treaded tire with snow", *SAE Int. J. Passeng. Cars – Mech.Syst.* 1 (2008), 1030-1038.

[5] Lee, J.H., Liu, Q., Mourelatos, Z.P., "Simulation of tire-snow interfacial forces for a range of snow densities with uncertainty", *SAE 2006 Transactions Journal of Materials and Manufacturing,* 398-407.

[6] Li, L., Sandu, C., Lee, J., Liu, B., "Stochastic modeling of tire-snow interaction using a polynomial chaos approach", *J. Terramechanics*, 46 (2009), 165-188.

[7] T. Muro, "Terramechanics. Land Locomotion Mechanics", A.A. Balkema Publishers, 2004.

[8] Schneebeli, M., Pielmeier, C., Johnson, J.B., "Measuring snow microstructure and hardness using a high resolution penetrometer", *Cold Regions Science and Technology,* 30 (1999), 101-114.

[9] Marshall, H.-P., Johnson, J., "Accurate inversion of high-resolution snow penetrometer signals for microstructural and micromechanical properties", *Journal of Geophysical Research – Earth Surface*, 114, F0401, 2009.

[10] Green, D., Korthauer, A., Way, J., "Validation of an Alaska Instrumented Vehicle", Senior Design Project Report, Department of Mechanical Engineering, University of Alaska Fairbanks, May 2010.